

## Magnetic-Moment Distributions in Ferromagnetic Ni-Cu Alloys\*

A. T. Aldred,<sup>†</sup> B. D. Rainford,<sup>‡</sup> T. J. Hicks,<sup>§</sup> and J. S. Kouvel<sup>¶</sup>

*Atomic Energy Research Establishment, Harwell, England*

(Received 9 August 1972)

The elastic diffuse scattering of neutrons from ferromagnetic Ni-Cu alloys of 2–40 at. % Cu has been measured at 4.2°K. Analysis of the results within the formalism of Marshall yields a description of the magnetic-moment distribution among the various atoms. The disturbance in moment produced by a copper atom at dilute concentrations appears to be confined almost completely to its nickel near neighbors, which is consistent with the short-range chemical screening effects predicted from coherent-potential theory. At higher copper concentrations, the moment disturbance extends over several neighbor shells, and it is argued that this longer-range effect is predominantly magnetic in origin. Inasmuch as the bulk moment per atom also contains a contribution from a uniform conduction-electron polarization  $\mu_{\text{cond}}$ , the average nickel and copper 3d moments  $\mu_{\text{Ni}}$  and  $\mu_{\text{Cu}}$  can only be determined in terms of the combinations  $\mu_{\text{Ni}} + \mu_{\text{cond}}$  and  $\mu_{\text{Cu}} + \mu_{\text{cond}}$ . The quantity  $\mu_{\text{Cu}} + \mu_{\text{cond}}$ , whose major component is probably  $\mu_{\text{cond}}$ , has a constant value of about  $-0.1\mu_B$  over the entire composition range studied.

### I. INTRODUCTION

Of the many contributions of neutron-diffraction experiments to our knowledge of magnetism in solids, none have answered a greater need than those that have provided information about atomic magnetic moments in transition-group metals and alloys. This has been particularly true in the complicated case of chemically disordered (solid-solution) alloys. The classic work of Shull and Wilkinson<sup>1</sup> has shown that neutron diffuse scattering data can yield a quantitative measure of the average magnetic moment of each atomic species in a binary ferromagnetic alloy. The Shull-Wilkinson technique is valid for all (concentrated as well as dilute) compositions and has been applied by many workers to a variety of magnetic alloy systems. Taken together, these experiments have revealed that the average magnetic moment of a transition-group atom (such as Ni) in an alloy is remarkably variable, its magnitude depending sensitively on the identity and concentration of the alloy constituents.

The variability of the *average* atomic moments with *over-all* alloy composition suggests that the magnetic moment of an *individual* atom may depend on its particular *local* environment in the alloy. Moreover, this local effect can produce a contribution to the neutron magnetic diffuse scattering cross section, which would cause a deviation from the atomic magnetic form factor at small scattering vectors. Recognizing this possibility, Low and his associates at Harwell developed a long-wavelength low-angle neutron diffractometer, which they have used to investigate local magnetic effects in a large number of alloy systems.<sup>2</sup> Until recently, however, the Harwell studies have been primarily confined to dilute alloys, for which the interpretation of the scattering data is relatively

simple.

In the case of dilute Ni-base alloys, it was discovered<sup>3</sup> that for a wide selection of non-transition-group solutes (Zn, Al, Ga, Si, Ge, Sn, Sb) each solute atom creates a magnetic disturbance in the surrounding nickel host, corresponding to a decrease in the local magnetization. Specifically, it was found that the magnitude of this disturbance depends on the electronic charge difference between the solute and nickel (i. e., it is smallest for Zn, and largest for Sb), and that it decays with increasing distance from a solute atom at approximately the same relative rate for all the solutes investigated, except possibly for zinc. Typically, the disturbance extends about 5 Å from a solute atom, thus affecting (i. e., lowering) the moments of the first four shells of neighboring nickel atoms. In the case of zinc, however, the neutron-scattering data indicate a somewhat shorter-ranged effect, which suggests that the magnetic disturbance in nickel may decrease in range when its magnitude falls below some threshold value. Hence, one might expect, if the solute in nickel were copper (where the charge difference would be even smaller than in Ni-Zn), that the magnetic disturbance would be weak and therefore confined to the immediate vicinity of each copper atom—which, in fact, is what we have found in the present study.

Our neutron-diffraction study of Ni-Cu is not restricted to the dilute-Cu alloys but extends almost completely across the ferromagnetic composition range (including the composition Ni<sub>80</sub>Cu<sub>20</sub>, the single Ni-Cu alloy whose magnetism has been studied previously by neutron diffraction<sup>4</sup>). Indeed, our interest in this alloy system derives not only from the previous work on dilute Ni-base alloys, but also from subsequent neutron-diffraction work at Harwell on some Ni-Cu alloys close to the critical composition for ferromagnetism (~56 at. %

Cu). The latter work<sup>5</sup> revealed that the spontaneous magnetization of these weakly ferromagnetic alloys is spatially distributed in giant polarization clouds with an average moment of  $\sim 10\mu_B$ . These results (and analogous results on Ni-Rh,<sup>5</sup> Ni-Pd,<sup>6</sup> and Ni-Cr<sup>7</sup>) closely resemble what was originally discovered in dilute PdFe alloys.<sup>8</sup> However, in PdFe every iron impurity atom is the nucleus of a polarization cloud, whereas in Ni-Cu relatively few of the nickel atoms (presumably only those with extremely Ni-rich local environments<sup>9</sup>) play this crucial role. Furthermore, in contrast to a palladium atomic moment in PdFe, whose magnitude depends primarily on its distance from an iron impurity atom, a nickel atomic moment in Ni-Cu can be expected to depend in magnitude not only on its distance from a polarization cloud nucleus but also on the many other statistical features of its local environment (i. e., the total number of nickel-atom neighbors and the magnitude of *their* moments).

The summary purpose of our measurements on Ni-Cu was the determination of the atomic moment variations as they evolve, with increasing copper in nickel, from isolated disturbances in the dilute alloys to some complex pattern of interacting effects which may be precursory to the polarization clouds that appear near the critical composition. In the interpretation of our neutron diffuse scattering data, we have relied on the analysis developed by Marshall,<sup>10</sup> which is valid for concentrated as well as dilute ferromagnetic alloys under certain prescribed conditions.<sup>11</sup>

## II. EXPERIMENTAL PROCEDURE

Ni-Cu alloy ingots of nominal composition, 2, 3, 6.2, 10, 20, 30, and 40 at.% Cu, were prepared by induction melting and chill casting under argon. All the ingots were severely cold rolled before being cut into appropriate samples for our magnetization and neutron-diffraction measurements. The polycrystalline samples were then annealed for 3 days at 1000 °C and water quenched. This mechanical and thermal treatment, similar to what was previously given to Ni-Cu alloys near the critical composition,<sup>5</sup> was meant to ensure macroscopic chemical homogeneity and a minimal amount of atomic clustering. It is known from previous neutron-diffraction work<sup>12</sup> that a clustering effect in Ni-Cu (predominantly between nearest-neighbor atoms) cannot be completely suppressed by sample quenching, and this has been borne out by our diffraction measurements, as will be shown later. Macroscopically, however, each of our samples is highly homogeneous, as evidenced by the sharp temperature dependence of the low-field magnetization observed near the Curie point.

Our magnetization measurements were made at the General Electric Research and Development Center on thin-disk samples mounted in a Foner-type vibrating-sample magnetometer and subjected to fields normal to the disk axis; the demagnetizing effect was therefore very small. At temperatures well below the Curie points of our alloy samples (the lowest of which is 163 °K for the 40 at.% Cu alloy), the high-field magnetization exhibited saturation plus a small differential susceptibility which was used to extrapolate linearly back to zero field and obtain the spontaneous magnetization. The spontaneous magnetization thus determined at 4.2 °K and its rate of change with alloy composition are two quantities that enter into the analysis of our neutron scattering data.

Our neutron scattering experiments were performed at Harwell with the diffractometer system mentioned earlier in this paper. The operation of this system, which has been described previously,<sup>13</sup> involves the time-of-flight detection of neutrons scattered elastically by the sample, which in our experiments was a Ni-Cu alloy slab (6 cm square and 6 mm thick) placed in the neutron beam with one of its long dimensions parallel to the scattering vector  $\vec{k}$ . The use of long-wavelength ( $\lambda \approx 4.8 \text{ \AA}$ ) neutrons allowed us to work at very small values of  $\kappa (= 4\pi\lambda^{-1} \sin\theta \approx 0.18\text{--}1.14 \text{ \AA}^{-1})$  in a practical range of scattering angles ( $2\theta \approx 7^\circ\text{--}52^\circ$ ); it also allowed us to avoid any multiple Bragg reflections. At each scattering angle (varied in increments of  $\sim 2^\circ$ ), the elastically scattered neutrons were counted during a time interval determined by a present number of incident neutrons. This counting cycle was repeated with the polycrystalline sample alternately in (a) a 4-kOe field applied parallel to  $\vec{k}$ , or (b) zero external field attained after field cycling; the latter condition represents a departure from the original operation of this system.<sup>13</sup> During cycle (a), since the magnetic moment of the entire sample is aligned parallel to  $\vec{k}$ , there is no magnetic scattering and only the nuclear scattering cross section is measured. During cycle (b), the sample is divided magnetically into many domains whose moments lie along the various easy magnetic axes of the randomly oriented crystallites; the scattering then consists of the entire nuclear component plus two-thirds of the maximum magnetic component (pertinent to complete moment alignment perpendicular to  $\vec{k}$ ). Hence, the difference between the scattered neutron counts during cycles (a) and (b) is solely a measure of the magnetic scattering cross section. The cross sections were placed on an absolute basis by comparison with the incoherent scattering from a thin plate of vanadium.<sup>14</sup> All our diffraction measurements were made with the samples at a temperature of 4.2 °K.

### III. EXPERIMENTAL RESULTS AND ANALYSES

#### A. Nuclear Diffuse Scattering

Our results for the nuclear part of the neutron scattering cross section will be presented first because the information on the atomic ordering or clustering in the alloy samples is needed for the analysis of our magnetic scattering data. Specifically, the expression we shall use for the magnetic diffuse scattering cross section includes a factor defined as

$$S(\kappa) = 1 + \sum_{R_i} \alpha(R_i) N(R_i) \sin \kappa R_i / \kappa R_i, \quad (1)$$

where  $R_i$  is the radius of the  $i$ th near-neighbor atomic shell,  $\alpha(R_i)$  is the chemical short-range order parameter for the  $i$ th shell (as defined by Cowley<sup>15</sup>),  $N(R_i)$  is the coordination number of the  $i$ th shell, and  $\kappa$  is the neutron scattering vector. This  $S(\kappa)$  factor also appears in the atomic disorder term which, together with an isotropic incoherent term, comprises the nuclear diffuse scattering cross section

$$\left( \frac{d\sigma}{d\Omega} \right)_{\text{nuc1}} = c \sigma_{\text{Cu}}^{\text{inc}} + (1-c) \sigma_{\text{Ni}}^{\text{inc}} + c(1-c) (b_{\text{Ni}} - b_{\text{Cu}})^2 S(\kappa). \quad (2)$$

This expression pertains to the alloy composition  $\text{Ni}_{1-c}\text{Cu}_c$ ; the  $\sigma$ 's are the incoherent scattering cross sections and the  $b$ 's are the coherent scattering lengths.

Thus,  $S(\kappa)$  can be determined from a measurement of  $(d\sigma/d\Omega)_{\text{nuc1}}$ , if the  $\sigma$ 's and  $b$ 's in Eq. (2) are known. Unfortunately,  $(d\sigma/d\Omega)_{\text{nuc1}}$  is dominated by the large incoherent contribution, particularly in the Ni-rich region, e.g., for  $c=0.1$ ,  $\sigma^{\text{inc}} \approx 345$ , whereas  $c(1-c)(b_{\text{Ni}} - b_{\text{Cu}})^2 \approx 7$ , in mb/sr atom. Therefore, small errors in the values of  $\sigma_{\text{Ni}}^{\text{inc}}$  and  $\sigma_{\text{Cu}}^{\text{inc}}$ , which are not accurately known, will produce very large systematic errors in the calculated  $S(\kappa)$ .

To obviate this problem in the determination of  $S(\kappa)$ , the following procedure was adopted. A best-fit curve of arbitrary shape was drawn through the experimental nuclear cross section for each alloy and extrapolated to  $\kappa = 1.2 \text{ \AA}^{-1}$ . The data and the fitted curves, including those for the 50 at.% Cu alloy studied earlier,<sup>5</sup> are presented in Fig. 1. From the analytical form of Eq. (1),  $S(\kappa)$  is expected to go through unity at  $\kappa \approx 1.2 \text{ \AA}^{-1}$  if the first-near-neighbor contribution is dominant (or even if the second-near-neighbor contribution is of comparable magnitude). The disorder term in the cross section was thus assumed to be known at this  $\kappa$  value and was subtracted from the experimental cross section. The remainder was then least-squares fitted as a function of alloy composition with  $\sigma_{\text{Cu}}^{\text{inc}}$  and  $\sigma_{\text{Ni}}^{\text{inc}}$  as parameters; the values obtained were  $\sigma_{\text{Cu}}^{\text{inc}} = 68 \pm 4$  and  $\sigma_{\text{Ni}}^{\text{inc}} = 376 \pm 3$ , in mb/

sr atom, both of which agree reasonably well with listed values.<sup>14</sup> The coherent scattering length values,  $b_{\text{Ni}} = 1.03$  and  $b_{\text{Cu}} = 0.76$ , in  $10^{-12}$  cm, were taken from Bacon's compilation.<sup>16</sup> These quantities were then inserted into Eq. (2) and the experimental cross-section data were converted to values of  $S(\kappa)$ , which are plotted in Fig. 2. These results were then least-squares fitted to Eq. (1), but this procedure was found to yield large unphysical values of  $\alpha(R_i)$  of alternating sign for successive atomic shells, which were probably caused by systematic errors in the data over this limited range of  $\kappa$ . Consequently, in order to increase the constraints in the fitting process, we used the experimental cross-section data in smoothed interpolated form as input and generated a series of  $S(\kappa)$  versus  $\kappa$  curves that closely matched the smoothed data curves. Moreover, the  $\alpha(R_i)$  values were chosen so that the ratios  $\alpha(R_i)/\alpha(R_1)$  stayed in good agreement with the ratios calculated from the  $\alpha(R_i)$  results of Mozer *et al.*<sup>12</sup> for a 52.5 at.% Cu alloy and from those of Cable *et al.*<sup>4</sup> for a 20 at.% Cu alloy. For other compositions, a continuous variation of  $\alpha(R_i)/\alpha(R_1)$  versus  $c$  was assumed, from which minor deviations were allowed to improve the fit between the generated and experimental curves for each alloy. This latter procedure enabled us to obtain  $\alpha(R_i)$  values that agreed reasonably well with previous results and represented a fit to our experimental data that was comparable to the original least-squares fit. In fact, the  $S(\kappa)$  versus  $\kappa$  curves for both fits lie within the thickness of the curves drawn in Fig. 2.

The numerical results of our analysis are listed in Table I, which also includes the results of earlier studies.<sup>4,12</sup> Inasmuch as the Ni-Cu alloys of the various investigations were subjected to somewhat different thermal and mechanical treatments (even though the common aim was to produce highly disordered alloys), an exact correspondence between the  $\alpha(R_i)$  values is not to be expected. Under these circumstances, the agreement is remarkably good. The same comments can be made about the different alloys of the present investigation, whose metallurgical treatments were nominally identical. Thus, when our  $\alpha(R_i)$  results are plotted against alloy composition, as shown in Fig. 3, they exhibit fairly smooth variations, but with deviations [particularly of the dominant  $\alpha(R_1)$ ] that probably reflect detailed metallurgical differences between the alloy samples.

From the convention adopted for the sign of  $\alpha(R_i)$ ,<sup>15</sup> a positive (or negative) value denotes a chemical clustering (or ordering) effect in which the relative number of  $i$ th-near-neighbor pairs of like (or unlike) atoms is larger than in a perfectly disordered alloy of the same average composition. Thus, from Table I and Fig. 3, it is evident that

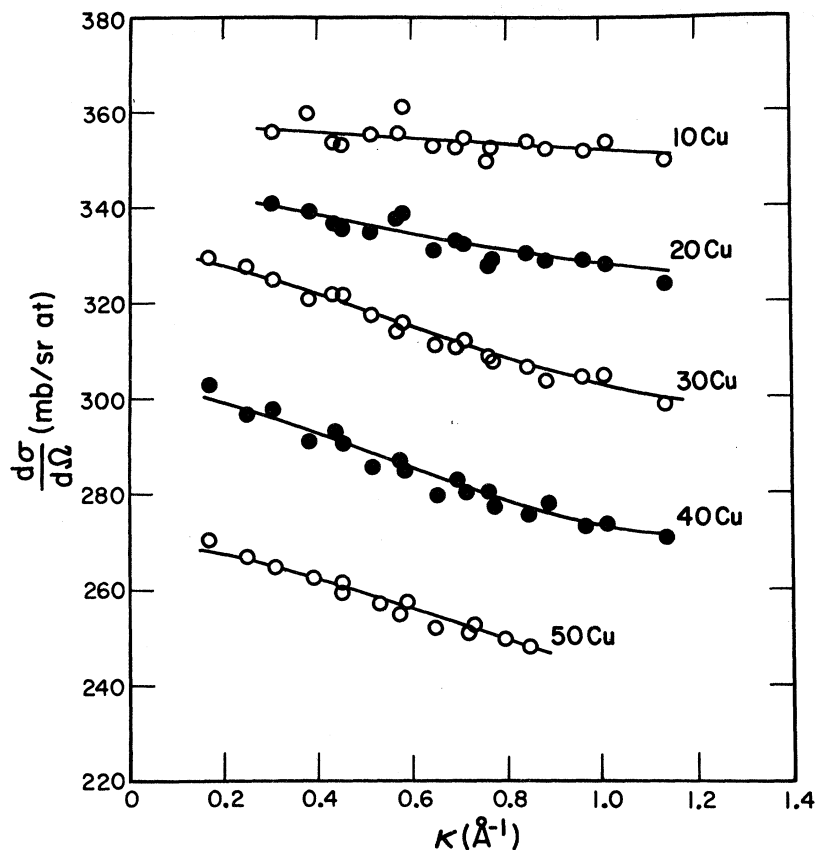


FIG. 1. Nuclear diffuse scattering cross sections  $d\sigma/d\Omega$  as a function of scattering vector  $\kappa$  for quenched Ni-Cu alloys.

the dominant chemical effect in our Ni-Cu alloy samples is a clustering of extremely short range. Furthermore, the variation of this atomic clustering effect with alloy composition, indicated by our results, appears to be consistent with the broad maximum at  $\sim 30$  at.% Cu in the positive enthalpy of mixing deduced from thermodynamic activity measurements on similar Ni-Cu alloys.<sup>17</sup>

The  $S(\kappa)$  vs  $\kappa$  curves determined by the  $\alpha(R_i)$  values in Fig. 3 form the normalizing bases for

the analyses of our magnetic scattering data presented below. For the 2.3 and 6.2 at.% Cu alloys, the scatter of our  $S(\kappa)$  results would have been prohibitively large, as can be seen from the trend of our results in Fig. 2. Consequently, for these two relatively dilute alloys, we used  $S(\kappa)$  vs  $\kappa$  curves constructed from  $\alpha(R_i)$  values taken from the curves in Fig. 3. This procedure is justified on the basis that these two alloys had received the same metallurgical treatment as all the others.

TABLE I. Chemical short-range order parameters for quenched Ni-Cu alloys determined from nuclear scattering data.

Conc. Cu	$\alpha(R_1)$	$\alpha(R_2)$	$\alpha(R_3)$	$\alpha(R_4)$	$\alpha(R_5)$	rms error
	$N(R_1) = 12$ $R_1 \approx 2.5 \text{ \AA}$	$N(R_2) = 6$ $R_2 \approx 3.5 \text{ \AA}$	$N(R_3) = 24$ $R_3 \approx 4.3 \text{ \AA}$	$N(R_4) = 12$ $R_4 \approx 5.0 \text{ \AA}$	$N(R_5) = 24$ $R_5 \approx 5.7 \text{ \AA}$	
0.10	0.055(10) <sup>a</sup>	0.048(15)	-0.005(7)	0.004(10)	0.002(4)	0.36
0.20	0.080(4)	0.062(7)	-0.007(3)	0.007(4)	0.006(2)	0.17
0.20 <sup>b</sup>	0.046(2)	0.039(8)	-0.010(3)	0.020(6)	...	...
0.30	0.118(2)	0.053(5)	-0.001(1)	0.009(2)	0.008(2)	0.09
0.40	0.103(3)	-0.001(6)	0.009(2)	0.009(3)	0.008(2)	0.11
0.50	0.106(2)	-0.009(4)	0.008(1)	0.007(2)	0.004(2)	0.07
0.525 <sup>c</sup>	0.121	-0.008	0.010	0.010	-0.001	...

<sup>a</sup>Numbers in parentheses represent statistical errors in last significant figure(s) of parameters.

<sup>b</sup>Cable *et al.* (Ref. 4).

<sup>c</sup>Mozer *et al.* (Ref. 12).

## B. Magnetic Diffuse Scattering

Our data for the magnetic part of the neutron diffuse scattering cross section are presented in Fig. 4. For the interpretation of these data, we follow the formal analysis of Marshall<sup>10</sup> and express the magnetic scattering cross section (in mb/sr atom) as<sup>18</sup>

$$\left(\frac{d\sigma}{d\Omega}\right)_{\text{magn}} = 48.6 c(1-c)S(\kappa)f^2(\kappa)[M(\kappa)]^2, \quad (3)$$

where

$$M(\kappa) = \mu_{\text{Cu}} - \mu_{\text{Ni}} + (1-c)G(\kappa) + cH(\kappa) \\ + (1-2c)[W(0) + W(\kappa)]. \quad (4)$$

In these expressions,  $c$  is the fractional concentration of copper,  $f(\kappa)$  is the atomic  $3d$  form factor, and  $\mu_{\text{Cu}}$  and  $\mu_{\text{Ni}}$  are the average  $3d$  magnetic moments of the copper and nickel atoms in the absence of any chemical short-range order. Furthermore,

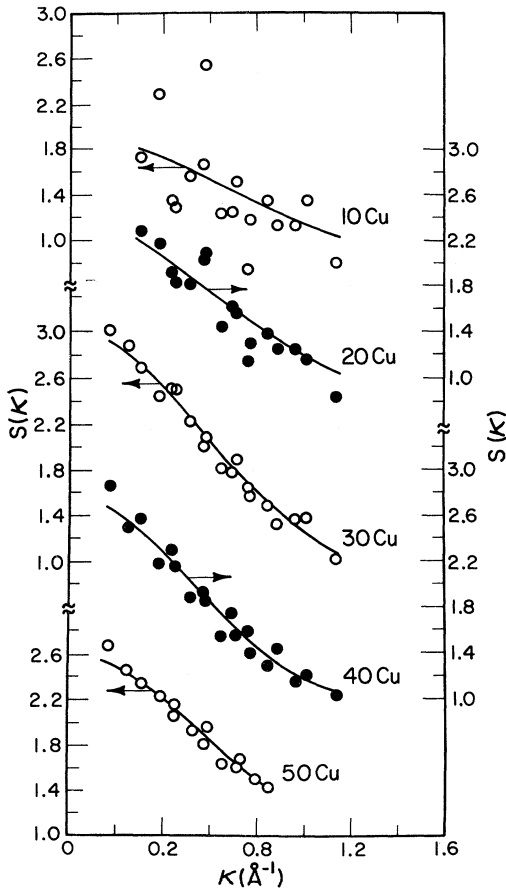


FIG. 2. Chemical short-range order function  $S(\kappa)$  as a function of scattering vector  $\kappa$ . The curves represent analytical fits to the data (see text).

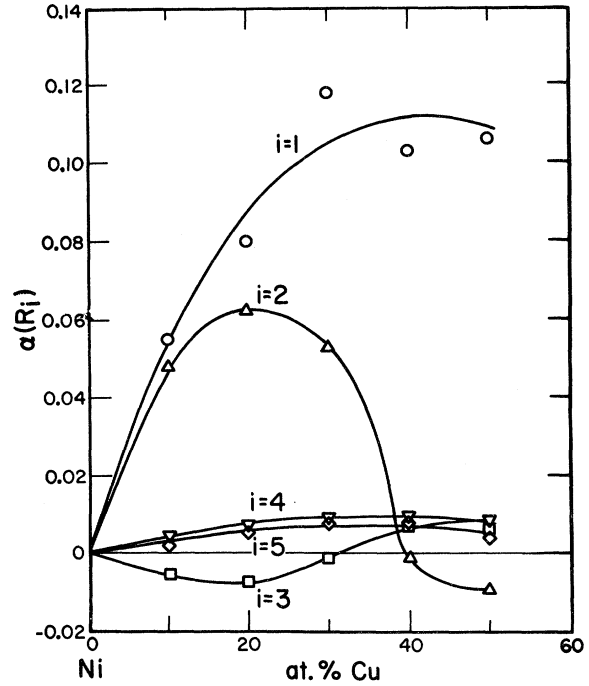


FIG. 3. Composition dependence of chemical short-range order parameters  $\alpha(R_i)$ .

$$G(\kappa) = \sum_{R_i} g(R_i)N(R_i) \frac{\sin \kappa R_i}{\kappa R_i}, \quad (5)$$

$$H(\kappa) = \sum_{R_i} h(R_i)N(R_i) \frac{\sin \kappa R_i}{\kappa R_i}, \quad (6)$$

and

$$W(\kappa) = \sum_{R_i} [h(R_i) - g(R_i)] \alpha(R_i)N(R_i) \frac{\sin \kappa R_i}{\kappa R_i}, \quad (7)$$

where  $g(R_i)$  represents the disturbance in the  $3d$  moment of a nickel atom caused by each additional copper atom at a distance  $R_i$ , and  $h(R_i)$  represents the corresponding disturbance in the  $3d$  moment of a copper atom. As before,  $N(R_i)$  is the coordination number and  $\alpha(R_i)$  the chemical short-range order parameter for the  $i$ th shell. It can be deduced from Marshall's work<sup>18</sup> that

$$\frac{d\langle \bar{\mu} \rangle}{dc} = M(0) = \mu_{\text{Cu}} - \mu_{\text{Ni}} + (1-c)G(0) + cH(0) \\ + 2(1-2c)W(0), \quad (8)$$

where  $\langle \bar{\mu} \rangle$  is the average atomic moment of an actual alloy with possibly some chemical short-range order. Since  $d\langle \bar{\mu} \rangle/dc$  can be determined separately by bulk magnetic measurement, Eq. (8) fixes the value that an experimental  $M(\kappa)$  versus  $\kappa$  curve should extrapolate to in the forward direction ( $\kappa=0$ ).

A substantial part of the  $\kappa$  dependence of the

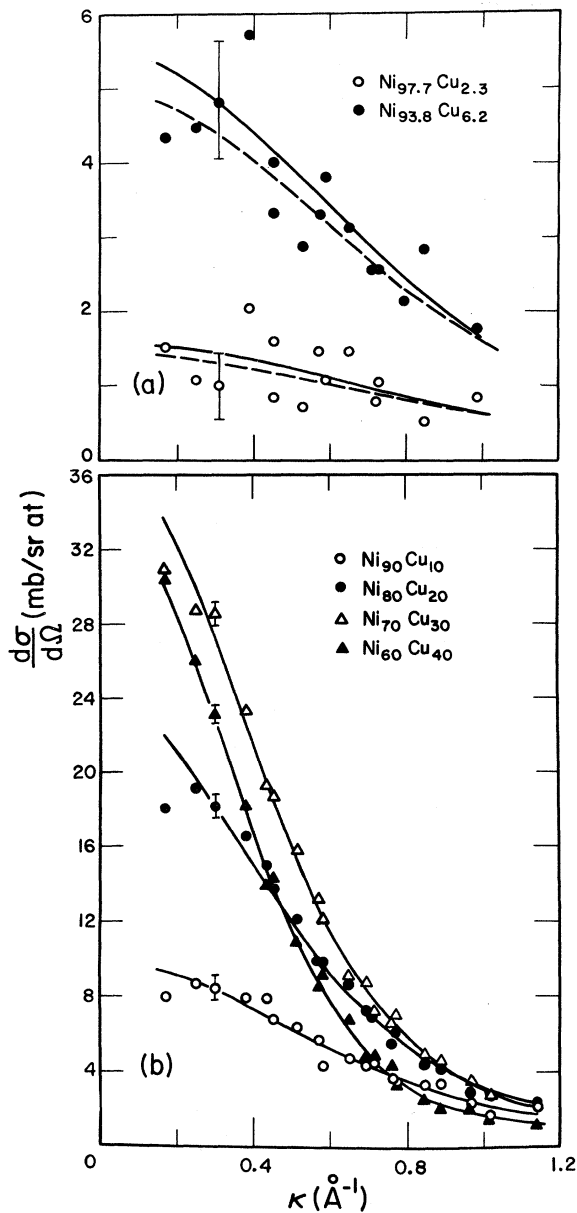


FIG. 4. Magnetic diffuse scattering cross sections as a function of scattering vector  $\kappa$ . The error bars denote typical statistical errors. The curves represent analytical fits to the data (see text).

magnetic scattering cross sections shown in Fig. 4 arises from that of  $S(\kappa)$ , for which our results were presented earlier. The weak  $\kappa$  dependence of the atomic  $3d$  form factor over our experimental range was approximated by the expression  $1 - 0.05\kappa^2$ , based on the calculated nickel form factor of Watson and Freeman,<sup>19</sup> which is consistent with the neutron Bragg scattering data of Mook.<sup>20</sup> Thus, by means of Eq. (3), values of  $M(\kappa)$  have been determined from the experimental cross sec-

tions, their negative sign fixed by the assumption that  $\mu_{\text{Ni}} > \mu_{\text{Cu}}$ ; these values are presented in Fig. 5. The large relative scatter of the data for the dilute alloys arises from the fact that the magnetic scattering cross section is small but the absolute error is the same, compared with the more concentrated alloys.

In principle, a set of  $M(\kappa)$  data fitted to Eqs. (4)–(7) should yield  $\mu_{\text{Cu}} - \mu_{\text{Ni}}$  and the  $\kappa$ -dependent terms involving  $g(R_i)$  and  $h(R_i)$ . Following Cable *et al.*<sup>4</sup> we assumed  $\mu_{\text{Cu}}$  is so small that  $h(R_i)$  can be neglected. Even then, our data are too restricted to allow a direct determination of all the  $g(R_i)$ 's. Many of the problems encountered earlier in the analytical fitting of the nuclear scattering

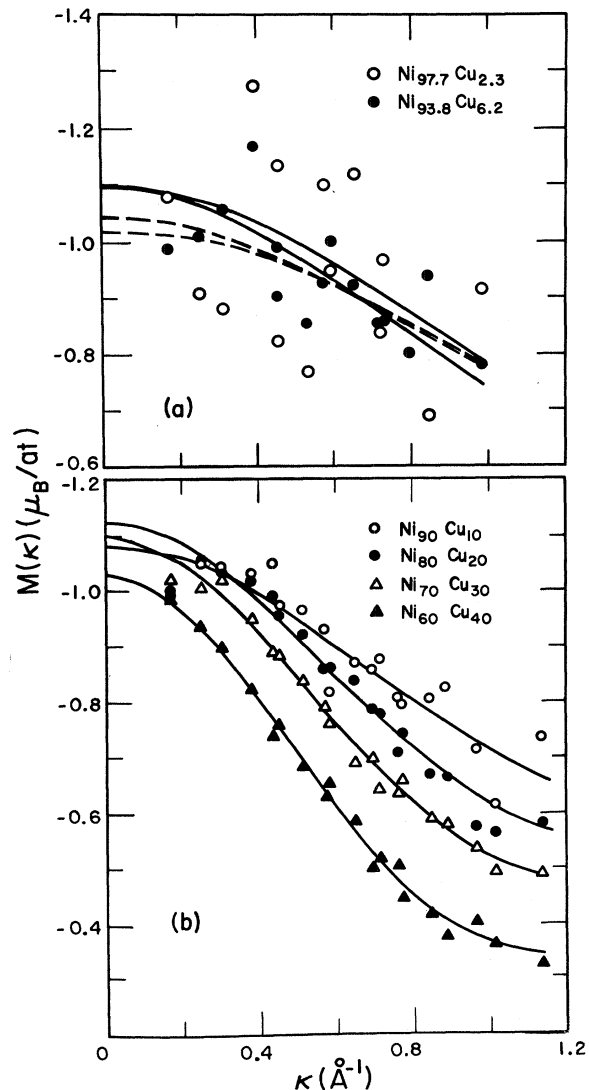


FIG. 5. Magnetic-moment density function  $M(\kappa)$  as a function of scattering vector  $\kappa$ . The curves represent analytical fits to the data (see text).

data were also present in the analysis of the magnetic scattering data, since similar  $\kappa$ -dependent functions are involved. Specifically, the rms error of the data analysis had a very shallow minimum which gave unrealistically large  $g(R_i)$  values of alternating sign for successive atomic shells. Accordingly, an additional constraint was imposed on the fitting routine, which corresponded to the minimization of the product of the rms error and the sum  $\sum_{R_i} |g(R_i)N(R_i)|$ . Each data point was weighted according to its statistical error. The number of parameters used in the fit was the smallest that would adequately represent the data. For all but the 2.3 and 6.2 at.% Cu alloys, this procedure resulted in a very satisfactory data fit, as shown by the curves in Figs. 4(b) and 5(b), and gave reasonably behaved values for the parameters, which are listed in Table II together with the parameter values of Cable *et al.* for a 20 at.% Cu alloy. The results of this analysis for the 2.3 and 6.2 at.% Cu alloys are indicated by the dashed curves in Figs. 4(a) and 5(a). The curves in the latter figure extrapolate to  $M(0)$  values of  $-1.046\mu_B$  and  $-1.021\mu_B$ , respectively, which depart considerably from the  $d\langle\bar{\mu}\rangle/dc$  value of about  $-1.14\mu_B$  deduced from our bulk magnetic measurements, as well as from the extrapolated  $M(0)$  values of about  $-1.10\mu_B$  for the adjacent concentrated alloys. Consequently, the fits for the two dilute alloys were further constrained to extrapolate to  $M(0) = -1.10\mu_B$ ; the results represented by the solid curves in Figs. 4(a) and 5(a) are clearly as consistent with the highly scattered data points as the dashed curves. The parameter values used for the solid curves are listed in Table II.

Our results for  $g(R_i)$  are plotted against alloy composition in Fig. 6. Owing to the large statistical errors in the higher-order  $g$ 's, only the  $g(R_1)$  values can be taken strictly at face value, and they are seen to be essentially constant over most of this composition range. Nevertheless, the

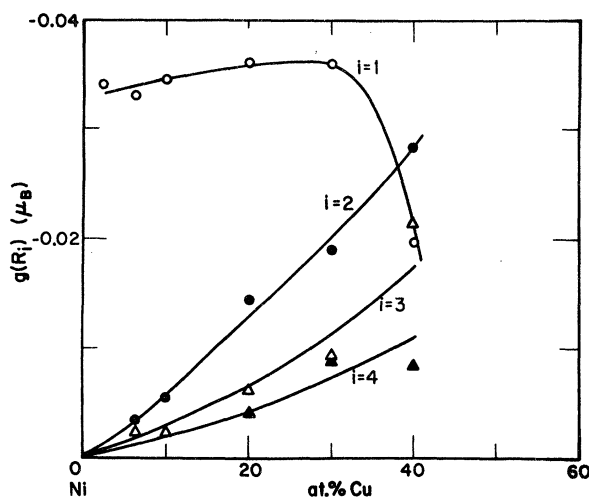


FIG. 6. Composition dependence of the nickel magnetic-moment disturbance parameters  $g(R_i)$ .

steady increase in magnitude of  $g(R_2)$  and  $g(R_3)$  with rising copper concentration undoubtedly reflects the increasingly more rapid decay of  $M(\kappa)$  with  $\kappa$  indicated by the data plots in Fig. 5. This change in the shape of  $M(\kappa)$  continues into the critical composition range.<sup>21</sup> Moreover, the quantity  $G(0)$ , defined in Eq. (5) as the sum of the  $g$ 's weighted by the coordination numbers, is a smooth (essentially linear) function of alloy composition, as seen in Fig. 7, which further supports the semi-quantitative validity of our higher-order  $g(R_i)$  values, especially when considered collectively. Although our  $g(R_1)$  value for the 20 at.% Cu alloy is in good agreement with that reported by Cable *et al.*, as seen in Table II, our higher-order  $g(R_i)$  values are larger in magnitude. Our data were obtained at lower  $\kappa$  values and should therefore give a more accurate determination of these higher-order components.

Our results for  $G(0)$  and the moment difference

TABLE II. Parameters (in  $\mu_B$ ) obtained from least-squares analyses of magnetic scattering cross sections of Ni-Cu alloys.

Conc. Cu	$\mu_{Cu} - \mu_{Ni}$	$g(R_1)$	$g(R_2)$	$g(R_3)$	$g(R_4)$	$G(0)$	$W(0)$	$\frac{d\langle\bar{\mu}\rangle}{dc}$ <sup>a</sup>	rms error
0.023	-0.706	-0.034				-0.409	0.006	-1.100	0.217
0.062	-0.684	-0.033	-0.003	-0.002		-0.473	0.016	-1.100	0.061
0.10	-0.665	-0.035	-0.006	-0.002		-0.508	0.025	-1.084	0.048
0.20	-0.602	-0.036	-0.014	-0.006	-0.004	-0.716	0.040	-1.125	0.026
0.20 <sup>b</sup>	-0.595	-0.038	-0.005	-0.006	0.001	-0.618	0.019	-1.066	0.027
0.30	-0.533	-0.036	-0.019	-0.009	-0.009	-0.875	0.058	-1.099	0.019
0.40	-0.426	-0.020	-0.028	-0.021	-0.009	-1.023	0.030	-1.028	0.020
Representative uncertainty	$\pm 0.010$	$\pm 0.002$	$\pm 0.013$	$\pm 0.006$	$\pm 0.010$	$\pm 0.015$	$\pm 0.005$	$\pm 0.025$	

<sup>a</sup>Derived from Eq. (8).

<sup>b</sup>Cable *et al.* (Ref. 4).

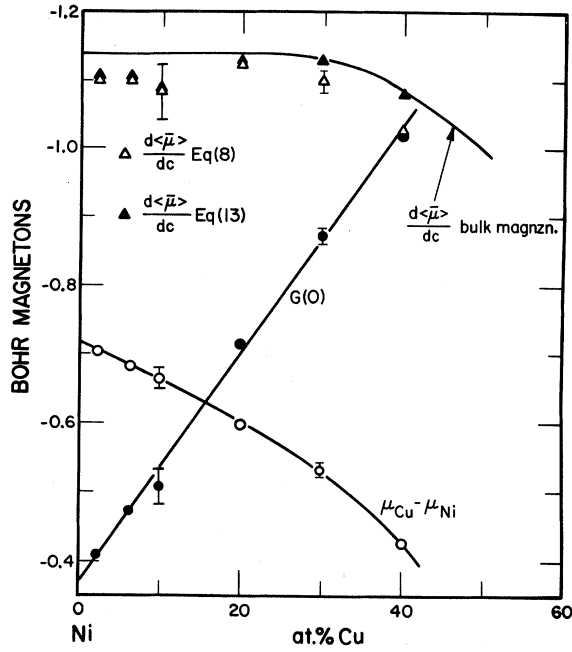


FIG. 7. Composition dependence of various parameters derived from magnetic neutron scattering data. Values of  $d\langle\bar{\mu}\rangle/dc$  determined from bulk magnetization measurements are shown for comparison. The error bars denote typical statistical uncertainties in the analytical fits to the data.

$\mu_{\text{Cu}} - \mu_{\text{Ni}}$  are plotted in Fig. 7; both vary smoothly with alloy composition but in opposite directions. According to Eq. (8),  $d\langle\bar{\mu}\rangle/dc$  depends additively on these two quantities and its values derived from this equation are fairly constant over most of the composition range, as shown in Fig. 7. A somewhat different expression for  $d\langle\bar{\mu}\rangle/dc$  can be derived from the basic definition

$$\langle\bar{\mu}\rangle = c\langle\mu_{\text{Cu}}\rangle + (1-c)\langle\mu_{\text{Ni}}\rangle, \quad (9)$$

where  $\langle\mu_{\text{Cu}}\rangle$  and  $\langle\mu_{\text{Ni}}\rangle$ , the atomic  $3d$  moments in the presence of chemical short-range order, are expressed by Marshall as<sup>22</sup>

$$\langle\mu_{\text{Cu}}\rangle = \mu_{\text{Cu}} + (1-c)\sum_{R_i} h(R_i)\alpha(R_i)N(R_i) \quad (10)$$

and

$$\langle\mu_{\text{Ni}}\rangle = \mu_{\text{Ni}} - c\sum_{R_i} g(R_i)\alpha(R_i)N(R_i). \quad (11)$$

Thus, Eq. (9) can be transformed to

$$\langle\bar{\mu}\rangle = c\mu_{\text{Cu}} + (1-c)\mu_{\text{Ni}} + c(1-c)W(0), \quad (12)$$

where  $W(0)$  is defined by Eq. (7). Differentiating Eq. (12) and noting that<sup>23</sup>  $d\mu_{\text{Ni}}/dc = G(0)$  and  $d\mu_{\text{Cu}}/dc = H(0)$ , we obtain

$$\frac{d\langle\bar{\mu}\rangle}{dc} = \mu_{\text{Cu}} - \mu_{\text{Ni}} + (1-c)G(0) + cH(0)$$

$$+ (1-2c)W(0) + c(1-c)\frac{dW(0)}{dc}. \quad (13)$$

The discrepancy between this expression and Eq. (8) can be traced to an implicit assumption<sup>24</sup> in the latter that all the  $\alpha(R_i)$ 's contained in  $W(\kappa)$  vary as  $c(1-c)$ ; under this condition Eq. (13) reduces to Eq. (8) exactly. Determining  $dW(0)/dc$  graphically and substituting its values and those of the other parameters [including  $H(0)=0$ ] into Eq. (13), we obtain the values of  $d\langle\bar{\mu}\rangle/dc$  shown in Fig. 7. The two sets of  $d\langle\bar{\mu}\rangle/dc$  values derived from the same neutron-scattering data diverge at copper concentrations beyond 20 at.%, and it can be seen from Fig. 3 that the dominant  $\alpha(R_i)$  parameter for our alloy samples departs from an approximate  $c(1-c)$  dependence in this same composition range. Our results for  $d\langle\bar{\mu}\rangle/dc$  derived from bulk magnetization data are also plotted in Fig. 7, and although they agree quite well with both sets of  $d\langle\bar{\mu}\rangle/dc$  values, they clearly favor those obtained from the more general expression, Eq. (13), at the higher copper concentrations. The  $d\langle\bar{\mu}\rangle/dc$  value obtained by Cable *et al.* for a 20 at.% Cu alloy (see Table II) is somewhat lower than any of our values for this composition, but the accuracy of their determination is probably affected by the longer extrapolation of their data to  $\kappa=0$ .

Values for the average atomic moment  $\langle\bar{\mu}\rangle$  determined from our low-temperature bulk magnetization measurements are presented in Table III and Fig. 8; they are in excellent agreement with previous experiments on Ni-Cu.<sup>25</sup> With these  $\langle\bar{\mu}\rangle$  values and the  $\mu_{\text{Cu}} - \mu_{\text{Ni}}$  and  $W(0)$  values derived from the neutron-scattering data, it might appear that Eq. (12) can be used to evaluate  $\mu_{\text{Ni}}$  and  $\mu_{\text{Cu}}$  separately. However, in addition to the terms indicated in Eqs. (9) or (12),  $\langle\bar{\mu}\rangle$  may also contain a spatially uniform component of the conduction-electron polarization, whose contribution to the neutron scattering cross section would be confined to values of  $\kappa$  well below the range of our experiments.<sup>26</sup> Although it should therefore not affect the interpretation of the neutron scattering data in terms of  $3d$ -band quantities, it must certainly be taken into account in any analysis in which these data are combined with those of bulk magnetic measurements. Thus, if we add a uniform conduction-electron moment per average atom ( $\mu_{\text{cond}}$ ) to the right-hand side of Eq. (12) and define

$$x = \langle\bar{\mu}\rangle - c(1-c)W(0) \quad (14)$$

and

$$y = \mu_{\text{Ni}} - \mu_{\text{Cu}} \quad (15)$$

in terms of the measurables [ $\langle\bar{\mu}\rangle$ ,  $\mu_{\text{Cu}} - \mu_{\text{Ni}}$ ,  $W(0)$ ], we find that

$$x + cy = \mu_{\text{Ni}} + \mu_{\text{cond}} \quad (16)$$

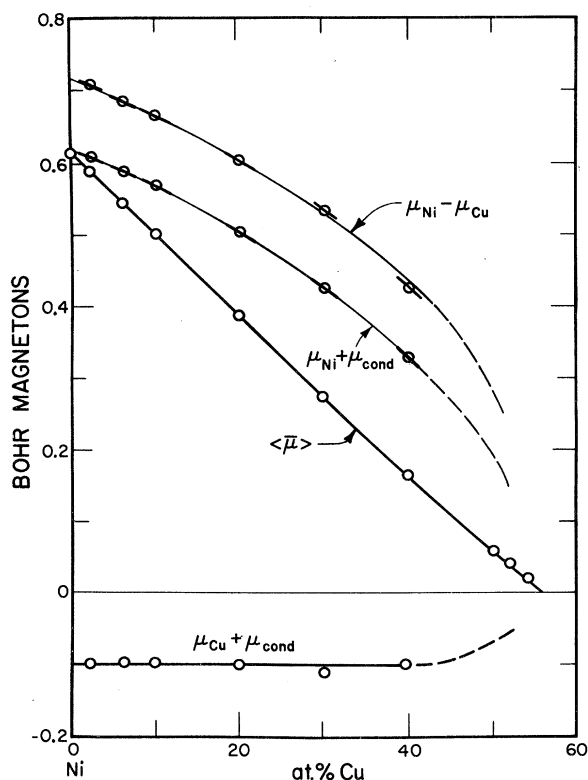


FIG. 8. Composition dependence of various combinations of average magnetic moments.

and

$$x - (1 - c)y = \mu_{Cu} + \mu_{cond} \quad (17)$$

Equations (16) and (17) show that neither of the  $3d$  moments,  $\mu_{Ni}$  or  $\mu_{Cu}$ , can be evaluated separately from the experimental information presently available to us. Nevertheless, these equations do allow us to determine the various moments in very simple combinations.

The quantities expressed in Eqs. (15)–(17) were evaluated for our Ni-Cu alloys and are listed in Table III; they are also plotted versus alloy composition in Fig. 8. The most striking feature of these results is the fact that  $\mu_{Cu} + \mu_{cond}$  has essentially the same negative value ( $\sim -0.10\mu_B$ ) over this wide composition range. Consequently, unless  $\mu_{Cu}$  and  $\mu_{cond}$  have large and exactly compensating composition dependences, which seems very unlikely, the steady decrease of the bulk alloy moment  $\langle \bar{\mu} \rangle$  with increasing copper concentration is almost entirely due to a decrease of the average  $3d$  moment of the nickel atoms. It would thus appear that in the above estimates of  $d\langle \bar{\mu} \rangle/dc$  from Eqs. (8) and (13), the assumption that the copper moment disturbance parameter  $H(0)$  is zero and the neglect of any composition dependence of  $\mu_{cond}$  are quite justified, and that the comparisons

with the slopes of  $\langle \bar{\mu} \rangle$  vs  $c$  are valid. With similar justification, the slopes of the  $\mu_{Ni} - \mu_{Cu}$  and  $\mu_{Ni} + \mu_{cond}$  curves in Fig. 8 (which are the same because the two curves are simply displaced vertically) can now be compared with the experimental values for  $G(0)$ , which should equal  $d\mu_{Ni}/dc$ , as noted earlier. The latter are represented in the figure by the short heavy lines drawn through the data points for the two curves. The close agreement between the slopes of these lines and those of the curves is further evidence that our data for Ni-Cu are quantitatively self-consistent. It should be noted, incidentally, that the linearity of  $G(0)$  vs  $c$  seen in Fig. 7 implies that the  $\mu_{Ni} - \mu_{Cu}$  and  $\mu_{Ni} + \mu_{cond}$  curves in Fig. 8 are simple parabolas over this composition range.

As indicated in Eq. (11), the average nickel  $3d$  moments in the actual alloy samples, namely,  $\langle \mu_{Ni} \rangle$ , may differ from  $\mu_{Ni}$  because of the existence of short-range chemical clustering. Inserting our  $\alpha(R_i)$  and  $g(R_i)$  values into this equation and calculating  $\langle \mu_{Ni} \rangle - \mu_{Ni}$ , we obtain the values listed in Table III. The values for this moment difference are all positive and reach a maximum at about 30 at.% Cu, thus reflecting the fact that the chemical clustering (which is largest at this composition) lowers the number of neighboring Ni-Cu atom pairs and therefore decreases the average disturbance (i. e., reduction) of the nickel moments. Inasmuch as our alloy samples are fairly close to perfect chemical disorder, it is not surprising that the calculated values for  $\langle \mu_{Ni} \rangle - \mu_{Ni}$  are very small. By suitable annealing, however, the amount of chemical clustering in these alloys can be raised substantially, and the consequent changes in various magnetic parameters such as  $\langle \mu_{Ni} \rangle - \mu_{Ni}$  would make an interesting future study.

#### IV. DISCUSSION

In Sec. III our magnetic diffuse neutron scattering data for Ni-Cu were presented and analyzed, following Marshall's scheme, in terms of parameters that represent various averages and local

TABLE III. Average magnetic moments (in  $\mu_B$ ) of Ni-Cu alloys.

Conc. Cu	$\langle \bar{\mu} \rangle$	$\mu_{Ni} - \mu_{Cu}$	$\mu_{Ni} + \mu_{cond}$	$\mu_{Cu} + \mu_{cond}$	$\langle \mu_{Ni} \rangle - \mu_{Ni}$
0.023	0.591	0.706	0.607	-0.099	0
0.062	0.545	0.684	0.587	-0.097	0.001
0.10	0.502	0.665	0.567	-0.098	0.002
0.20	0.388	0.602	0.502	-0.100	0.008
0.20 <sup>a</sup>	0.377	0.596	0.496	-0.100	0.004
0.30	0.275	0.533	0.423	-0.110	0.017
0.40	0.166	0.426	0.329	-0.097	0.012
Representative uncertainty	$\pm 0.0005$	$\pm 0.010$	$\pm 0.010$	$\pm 0.010$	$\pm 0.001$

<sup>a</sup>Cable *et al.* (Ref. 4).

disturbances of atomic magnetic moments. Moreover, when tested internally and against appropriate bulk properties, these parameters were shown to give a consistent formal description of the low-temperature ferromagnetic state of these alloys on an atomic scale. For the remainder of this paper, we will discuss two major aspects of this formal picture and suggest possible physical interpretations.

The aspect of our results that serves the main purpose of this study is illustrated in Fig. 6, where the magnetic disturbance parameters  $g(R_i)$  are plotted against alloy composition. At dilute copper concentrations, where only  $g(R_1)$  is of significant magnitude, the situation is clearly very simple. In these dilute alloys, the magnetic disturbance produced by a copper solute atom is strictly confined to its nickel near-neighbor atoms and corresponds to a small ( $\sim 5\%$ ) reduction of each of their moments. As mentioned at the outset, similar neutron-diffraction experiments on other Ni-base alloys<sup>3</sup> have suggested a trend toward a weaker and shorter-ranged moment disturbance as the charge difference between solute and nickel host becomes smaller. In Ni-Cu, where the charge difference is down to one electron per atom, this trend has now been shown to reach an extreme limit. It would appear that the electronic screening of the larger nuclear charge of copper is accomplished almost completely within each copper atomic cell, with only a small residue of the screening charge extending as far as the nickel near neighbors, the rest of the nickel host remaining essentially unaffected. Thus, for the dilute-Cu alloys at least, our results are consistent with recent photoemission studies<sup>27,28</sup> which indicate that the electronic density of states of a Ni-Cu alloy resembles that of a mixture of the two pure elements, in agreement with various coherent-potential models,<sup>29,30</sup> rather than that of an intermediate pseudoelement considered from the collective-electron rigid-band viewpoint.

The moment reduction on a nickel atom adjacent to a copper atom probably arises predominantly from the chemical screening effect just described, and partly from a direct magnetic effect resulting from the replacement of one of its moment-bearing nickel neighboring atoms by a copper atom with little or no moment. Another possible contributor to this moment reduction is a cooperative magnetic effect deriving from the fact that the nickel atom is also adjacent to several other nickel near neighbors (with moments similarly reduced) of the same copper atom, and its moment is thereby further reduced. In any case, as we see in Fig. 6, the total near-neighbor effect is a  $g(R_1)$  that remains remarkably constant out to about 30 at.% Cu, which would suggest that over this wide composition range

the nickel moment disturbance depends linearly on the number of copper near neighbors, thus complying with the basic simplifying assumption of the Marshall analysis.<sup>11</sup> However, we also see in Fig. 6 that the higher-order  $g(R_i)$ 's increase steadily in magnitude over the same composition range, indicating that these longer-ranged moment disturbances probably do not obey the Marshall linearity condition.<sup>21</sup> It is unlikely that the ranges of the chemical screening and direct magnetic effects change appreciably with alloy composition, but the fact that second and third near-neighbor Ni-Cu atom pairs (like the adjacent Ni-Cu pairs described above) have near-neighbor nickel atoms in common can produce magnetic disturbances that are cooperative and nonlinear. Hence, the rapid increase of  $g(R_2)$  and  $g(R_3)$  relative to  $g(R_1)$  at high copper concentrations is probable evidence of cooperative magnetic effects which grow and ultimately define the boundaries of the extended polarization clouds observed near the critical composition.<sup>5</sup>

The other aspect of our results that deserves further comment concerns the average atomic moments (in combination) and their variation with alloy composition, which are presented in Table III and in Fig. 8. The fact that  $\mu_{Cu} + \mu_{cond}$  is a sizable negative quantity that remains remarkably constant over a wide composition range raises several intriguing questions. Most of all, we should like to know the separate contributions of  $\mu_{Cu}$  and  $\mu_{cond}$  to this combined quantity because this information would allow us to extract  $\mu_{Ni}$  from our results for  $\mu_{Ni} - \mu_{Cu}$  for each alloy. In the case of pure nickel, Mook<sup>20</sup> has fitted his neutron Bragg scattering data with a  $3d$  magnetic form-factor curve calculated for the free nickel atom and, from this fit, deduced a  $3d$  moment ( $\mu_{Ni}$ ) of  $0.711\mu_B$  and a negative uniform polarization ( $\mu_{cond}$ ) of  $-0.105\mu_B$ ,<sup>31</sup> where the scattering produced by the latter was presumed to occur at  $\kappa = 0$  and thus be unobservable. A simple extension of this interpretation to our Ni-Cu results (and to those of Cable *et al.*<sup>4</sup>) would strongly imply that the value of  $\sim -0.10\mu_B$  obtained for  $\mu_{Cu} + \mu_{cond}$  is solely due to  $\mu_{cond}$  and, consequently, that the  $3d$  polarization of copper ( $\mu_{Cu}$ ) is extremely small. This would be consistent with the photoemission work on Ni-Cu,<sup>27,28</sup> which suggests that the copper contribution to the  $3d$  density of states lies well below the Fermi level and is therefore occupied by electrons of balanced spin. The absence of a copper  $3d$  moment in Ni-Cu alloys has also been claimed on the basis of nuclear magnetic relaxation measurements.<sup>32</sup>

However, a less extreme interpretation is not excluded since Mook's diffraction data on nickel do allow an extrapolation to a somewhat lower  $3d$  form factor at  $\kappa = 0$  than that obtained from the free-atom fit, and this would yield a smaller  $\mu_{Ni}$

and, therefore, a smaller negative value for  $\mu_{\text{cond}}$ . The  $\mu_{\text{Cu}} + \mu_{\text{cond}}$  results for Ni-Cu can then be taken to contain a significant (though probably small) negative value of  $\mu_{\text{Cu}}$ . This possibility is also allowed by the fact suggested earlier that the electronic screening charge about each copper atom persists somewhat outside the atomic cell, which could cause the copper  $3d$  band to extend up to the Fermi level, where an exchange splitting would result in a magnetic moment.

Whatever the relative proportions of  $\mu_{\text{Cu}}$  and  $\mu_{\text{cond}}$  may be, the variation of the experimental quantity  $\mu_{\text{Cu}} + \mu_{\text{cond}}$  with alloy composition remains a separate question of interest. Since  $\mu_{\text{Cu}}$  and  $\mu_{\text{cond}}$  may each be regarded as a magnetic polarization induced by exchange interactions with the  $3d$  moments of the nickel atoms, it seems reasonable to expect  $\mu_{\text{Cu}} + \mu_{\text{cond}}$  to scale roughly with  $\mu_{\text{Ni}}$ , the average nickel  $3d$  moment. If the small contribution of  $\mu_{\text{Cu}}$  to  $\mu_{\text{Ni}} - \mu_{\text{Cu}}$  is ignored, it is seen in

Fig. 8 that  $\mu_{\text{Ni}}$  decreases by  $\sim 40\%$  over the composition range 0–40 at.% Cu. Yet, despite this large change in  $\mu_{\text{Ni}}$ , the quantity  $\mu_{\text{Cu}} + \mu_{\text{cond}}$  remains essentially constant, which suggests that the creation of at least its dominant component (presumably  $\mu_{\text{cond}}$ ) involves some limiting or saturation process.

#### ACKNOWLEDGMENTS

We are extremely grateful to Dr. J. W. Garland for many enlightening discussions concerning the physical interpretation of our results, particularly regarding various intricacies of the Marshall formalism. We also thank Dr. G. G. Low, Dr. F. Y. Fradin, and Dr. J. B. Comly (as well as Dr. Garland) for their helpful suggestions concerning this paper, and V. Rainey and H. F. Burne for their capable assistance in the neutron scattering and bulk magnetic measurements, respectively.

\*Work performed in part under the auspices of the U. S. Atomic Energy Commission.

†On assignment from Argonne National Laboratory, Argonne, Ill. 60439 (permanent address).

‡On attachment from Imperial College, London, England.

§Present address: Monash University, Clayton, Victoria, Australia.

¶On leave from General Electric Research and Development Center, Schenectady, N. Y. Present address: Department of Physics, University of Illinois, Chicago, Ill. 60680.

<sup>1</sup>C. G. Shull and M. K. Wilkinson, *Phys. Rev.* **97**, 304 (1955).

<sup>2</sup>G. G. Low, *J. Appl. Phys.* **39**, 1174 (1968); *Advan. Phys.* **18**, 371 (1969), and references therein.

<sup>3</sup>J. B. Comly, T. M. Holden, and G. G. Low, *J. Phys. C* **1**, 458 (1968).

<sup>4</sup>J. W. Cable, E. O. Wollan, and H. R. Child, *Phys. Rev. Letters* **22**, 1256 (1969).

<sup>5</sup>T. J. Hicks, B. Rainford, J. S. Kouvel, G. G. Low, and J. B. Comly, *Phys. Rev. Letters* **22**, 531 (1969).

<sup>6</sup>A. T. Aldred, B. D. Rainford, and M. W. Stringfellow, *Phys. Rev. Letters* **24**, 897 (1970).

<sup>7</sup>B. D. Rainford, A. T. Aldred, and G. G. Low, *J. Phys. (Paris)* **32**, C1-575 (1971).

<sup>8</sup>G. G. Low and T. M. Holden, *Proc. Phys. Soc. (London)* **89**, 119 (1966).

<sup>9</sup>J. S. Kouvel and J. B. Comly, *Phys. Rev. Letters* **24**, 598 (1970).

<sup>10</sup>W. Marshall, *J. Phys. C* **1**, 88 (1968).

<sup>11</sup>The main restriction of Marshall's analysis (Ref. 10) is the assumption that in a binary alloy (e.g., Ni-Cu) the magnetic moment of a nickel or copper atom varies linearly with the number of copper atoms at a given distance. This linearity assumption was later relaxed by E. Balcar and W. Marshall [*J. Phys. C* **1**, 966 (1968)] but the results of their analysis are too complicated for our present purposes.

<sup>12</sup>B. Mozer, D. T. Keating, and S. C. Moss, *Phys. Rev.* **175**, 868 (1968).

<sup>13</sup>G. G. Low and M. F. Collins, *J. Appl. Phys.* **34**, 1195 (1963).

<sup>14</sup>G. E. Bacon, *Neutron Diffraction* (Clarendon, Oxford, England, 1962), 2nd ed., p. 31.

<sup>15</sup>J. M. Cowley, *Phys. Rev.* **77**, 669 (1950).

<sup>16</sup>G. E. Bacon, *Acta Cryst.* **A25**, 391 (1969).

<sup>17</sup>R. A. Rapp and F. Maak, *Acta Met.* **10**, 63 (1962).

<sup>18</sup>In Eq. (3), the numerical coefficient 48.6 equals the constant  $(\gamma e^2/2mc^2)^2$  times  $\frac{2}{3}$ , which derives from the on-off application of the magnetic field during the scattering measurements. The function  $S(\kappa)$  defined in Eq. (1) equals  $1 + S_M(\kappa)/c(1-c)$ , where  $S_M(\kappa)$  is the  $S$  function used by Marshall (Ref. 10). Analogously, the function  $W(\kappa)$ , defined in Eq. (7), equals  $W_M(\kappa)/c(1-c)$ , where  $W_M(\kappa)$  is Marshall's  $W$  function. A similar procedure was adopted by Cable *et al.* (Ref. 4).

<sup>19</sup>R. E. Watson and A. J. Freeman, *Acta Cryst.* **14**, 27 (1961).

<sup>20</sup>H. A. Mook, *Phys. Rev.* **148**, 495 (1966).

<sup>21</sup>The earlier neutron magnetic scattering data for the 50 at.% Cu alloy (Ref. 5) show a decay of  $M(\kappa)$  with  $\kappa$  that is so rapid that our Marshall-type analysis gives essentially zero for  $g(R_1)$  through  $g(R_3)$  with all the moment disturbance appearing in a  $g(R_4)$  of about  $-0.1\mu_B$ . In this truncated analysis, the  $g(R_4)$  value probably contains contributions from  $g$ 's of still higher order. Furthermore, even though this analysis produces a reasonable fit to the data points, extrapolation of the analytical curve to  $\kappa=0$  gives a  $d\langle\mu\rangle/dc$  value that is about 20% smaller in magnitude than that deduced from bulk magnetization data. It therefore appears that the Marshall model has truly broken down in this critical composition region.

<sup>22</sup>Equations (10) and (11) are equivalent to Eqs. (7.15) and (7.16) in Ref. 10.

<sup>23</sup>These expressions which are identical to Eqs. (6.13) and (6.14) in Ref. 10 can be shown to be valid even in the presence of short-range chemical order.

<sup>24</sup>The equivalent assumption was implicitly made by Marshall (Ref. 10) that his function  $s(R)$  varies as  $c^2(1-c)^2$ .

<sup>25</sup>S. A. Ahern, M. J. C. Martin, and W. Sucksmith,

Proc. Roy. Soc. (London) **A248**, 145 (1958).

<sup>26</sup>If there is any nonuniform component of the conduction-electron polarization that varies from nickel site to copper site, it would presumably follow approximately a  $3d$  form factor and would therefore combine with the average  $3d$  moments  $\mu_{Ni}$  and  $\mu_{Cu}$ .

<sup>27</sup>D. H. Seib and W. E. Spicer, Phys. Rev. B **2**, 1694 (1970).

<sup>28</sup>S. Hüfner, G. K. Wertheim, R. L. Cohen, and J. H. Wernick, Phys. Rev. Letters **28**, 488 (1972).

<sup>29</sup>S. Kirkpatrick, B. Velický, and H. Ehrenreich, Phys.

Rev. B **1**, 3250 (1970).

<sup>30</sup>G. M. Stocks, R. W. Williams, and J. S. Faulkner, Phys. Rev. Letters **26**, 253 (1971); Phys. Rev. B **4**, 4390 (1971).

<sup>31</sup>Mook's numerical results are based on  $0.606\mu_B/\text{atom}$  as the bulk saturation moment of nickel at  $0^\circ\text{K}$ , whereas the currently accepted value (the standard for our  $\langle\mu\rangle$  results listed in Table III) is  $0.616\mu_B/\text{atom}$ . See H. Danan, A. Herr, and A. J. P. Meyer, J. Appl. Phys. **39**, 669 (1968).

<sup>32</sup>M. H. Bancroft, Phys. Rev. B **2**, 182 (1970).

## Evidence for a Second Magnetic Phase Transition in Gadolinium\*

M. B. Salamon<sup>†</sup> and D. S. Simons

*Department of Physics and Materials Research Laboratory, University of Illinois, Urbana, Illinois 61801*

(Received 24 April 1972)

The heat capacity and temperature derivative of the electrical resistivity of Gd have been measured simultaneously in the vicinity of 226 K, where the easy axis of magnetization tilts away from the crystallographic  $c$  axis. In addition to the known anomaly in the  $a$ -axis resistivity, a small step change in the specific heat was observed. Application of magnetic fields above 1000 Oe along the  $c$  axis or 120 Oe along the  $a$  axis suppressed both the resistive and specific-heat anomalies. This behavior is discussed in terms of a molecular-field model which treats the anisotropy energy as a term in the magnetic free energy. The tilting of the easy axis is driven by the temperature dependence of the magnetization, which causes the lowest-order anisotropy constant  $K_1$  to change sign. The magnitudes of the step in the specific heat and the critical field in the  $c$ -axis direction calculated in this model are in good agreement with experiment.

Gadolinium has long been considered a simple ferromagnet below its Curie temperature of 291 K, although its easy magnetization axis is known to vary with temperature. The magnetization is aligned with the hexagonal  $c$  axis just below  $T_C$ , but tilts away from it to form a cone below a temperature of 220–240 K.<sup>1–3</sup> In this same temperature range, anomalies have been found in many magnetic, thermal, and electrical properties of gadolinium, including the magnetization,<sup>4,5</sup> magnetostriction,<sup>6,7</sup> thermal expansion,<sup>7</sup> elastic constants,<sup>8,9</sup> electrical resistance,<sup>10</sup> and magneto-resistance.<sup>11</sup> We report here a simultaneous measurement of the specific heat and temperature derivative of the electrical resistance of gadolinium between 213 and 243 K and attempt to clarify the nature of the anomalous behavior by means of a simple molecular-field model.

An ac calorimetry technique which has been previously described<sup>12</sup> was used to make the measurements. The sample of gadolinium was a single crystal cut from the same source used by Lewis to measure the specific heat near the Curie point,<sup>13</sup> and was estimated to have 0.1% rare-earth impurities and 0.5% other impurities. It was cut to dimensions  $7.0 \times 1.5 \times 0.1 \text{ mm}^3$ , with the  $7.0$ -

mm side parallel to the  $a$  axis and the  $1.5$ -mm side parallel to the  $c$  axis. The sample was annealed between two tantalum sheets in a vacuum of  $5 \times 10^{-6}$  Torr for 24 h at  $850^\circ\text{C}$ . Tantalum current and voltage leads were spot welded such that the current was directed along the  $a$  axis. Measurements were made in magnetic fields applied along the  $a$  or  $c$  axis. Since the field was always in the plane of the sample, demagnetizing effects were negligible.

In Fig. 1(a) we have plotted the results of specific-heat measurements made with fields applied along the  $c$  axis. In zero field, a step change in the specific heat is observed at 226 K with a value

$$\Delta C_p = 0.09 \pm 0.01 \text{ cal/mole K.} \quad (1)$$

Increasing the field decreases the size of the specific-heat anomaly, and it apparently disappears between 0.7 and 1.0 kOe.

The temperature derivative of resistance shown in Fig. 1(b) provides a more sensitive measure of the presence of a transition. Behavior which strongly suggests spin-disorder scattering<sup>14,15</sup> is observed in zero field. Application of the magnetic field shifts the peak to lower temperatures, distorts its shape, and finally suppresses it com-